

## Impact-Parameter Dependence of Vacancy Production in Strongly Bound Quasimolecular States of Heavy Collision Systems

J. S. Greenberg

*Gesellschaft für Schwerionenforschung, D-6100 Darmstadt 1, West Germany, and A. W. Wright Nuclear Structure Laboratory, Yale University, New Haven, Connecticut 06520*

and

H. Bokemeyer, H. Emling, E. Grosse, and D. Schwalm

*Gesellschaft für Schwerionenforschung, D-6100 Darmstadt 1, West Germany*

and

F. Bosch

*Max-Planck-Institut für Kernphysik, D-6900 Heidelberg 1, West Germany*

(Received 19 September 1977)

With a new method to determine the impact-parameter dependence,  $P(\rho)$ , of  $K$ -shell vacancy production, which utilizes a kinematic analysis of Doppler-broadened x-ray lines, we show that the  $K$ -shell excitation probability in heavy collision systems at Coulomb barrier energies is both large and narrowly peaked at small impact parameters. In particular, for  $1s\sigma$  excitations,  $P(\rho \approx 0)$  can exceed a few percent with approximately half the total cross section contributed by collisions with  $\rho \lesssim 40$  fm.

The current search<sup>1</sup> for the predicted positron decay<sup>2</sup> of strongly bound quasimolecular hole states in heavy collision systems has focused attention on the associated  $K$ -shell ionization required to observe some of these more interesting aspects of the unusually strong electronic binding expected in superheavy atoms. Not only is the magnitude of the cross section for vacancy production in the deepest-lying molecular level, the  $1s\sigma$  state, a central consideration in most of the experiments, but because of the dominant one-collision nature of the production and decay processes, the feasibility of observing these phenomena depends critically on establishing that a significant part of the excitation probability is produced by small-impact-parameter collisions where the energy levels are most strongly bound. Recent calculations by Betz *et al.*<sup>3</sup> have demonstrated that the same relativistic energy-level structure which is being sought in the positron search experiments<sup>1</sup> qualitatively modifies the previous small estimates<sup>4,5</sup> ( $10^{-4}$ – $10^{-5}$ ) for the excitation probability at zero impact parameter,  $P(\rho = 0)$ , extrapolated from light systems. These small limits would certainly have relegated the above-mentioned positron-decay experiments to failure.

In this Letter we present the first results of a determination of the impact-parameter dependence,  $P(\rho)$ , for  $K$ -shell vacancy production in collisions where relativistic effects are expected

to contribute significantly. We show that  $P(\rho \approx 0)$  is, indeed, as large as a few percent for  $1s\sigma$  vacancy production in heavy collision systems, and that a substantial part of this cross section is contributed by impact parameters  $\rho \lesssim 40$  fm. A method of measuring  $P(\rho)$  is introduced which exploits the one-to-one correspondence between the differential cross section and the Doppler-broadened line shapes of both the target and projectile characteristic x rays observed at  $0^\circ$  relative to the beam direction.<sup>6</sup> It is particularly sensitive to probing the small-impact-parameter dependence of  $P(\rho)$  where the relativistic effects are most important. The feasibility of this technique was initially demonstrated by Greenberg *et al.*<sup>7</sup> Recently Anholt<sup>8</sup> and Behncke *et al.*<sup>9</sup> fitted the shape of Doppler-broadened lines, observed for angles other than  $0^\circ$  in heavy collision systems, with analytic functions for  $P(\rho)$ .

The main features of the relationship between the impact parameter and the observed photon energy are readily illustrated. With the detector located at  $0^\circ$ , the Doppler shift,  $\Delta E_x$ , for an x-ray of energy  $E_{x0}$  emitted by the projectile or target is given to first order in the velocity by,

$$\Delta E_x = (E_{x0} v_{c.m.}/c) [1 + (-1)^{i+1} K_i \cos \theta_i], \quad (1)$$

independent of the azimuthal scattering angle. Here  $v_{c.m.}$  is the center-of-mass velocity;  $\theta_i$  is the scattering angle of the projectile in the c.m. system;  $i = 1$  and  $2$  refer to projectile and target,

respectively;  $K_1 = A_1/A_2$  and  $K_2 = 1$ . The line shapes reflect a particularly simple analytic form for this case of azimuthal symmetry and for isotropic emission of the  $K$  x ray<sup>6</sup>:

$$\frac{d[N(\Delta E_x)]}{d(\Delta E_x)} = \frac{2\pi c}{E_{x0} v_{c,m,K_i}} P[\rho(\Delta E_x)] \frac{a^2}{4} \left[ 1 + \left( \frac{\rho(\Delta E_x)}{a} \right)^2 \right]^2 \left( \frac{E_x}{E_{x0}} \right)^2 \xi(E_x), \quad (2)$$

where  $\xi(E_x)$  is the photon frequency response of the detector at  $E_{x0} + \Delta E_x$ , and  $a$  is half the distance of closest approach in a head-on collision. Equation (2), correct to first order in  $v/c$ , clearly displays the one-to-one relation between the impact-parameter dependence and the photon energy observed at  $0^\circ$ . The  $0^\circ$  observation angle is unique in this respect. This essential feature is rapidly lost as the detector is moved away from the forward observation angle. However, at the larger observation angles, and particularly at  $90^\circ$ , there exists an increased sensitivity to larger impact parameters over that available at  $0^\circ$ ; this can yield valuable complementary information for larger  $\rho$  values.

The measurements reported herein were carried out with  $^{136}\text{Xe}$  and  $^{238}\text{U}$  beams from the GSI (Gesellschaft für Schwerionenforschung) Unilac at energies of 4.7 MeV/amu. In order to observe the x rays at  $0^\circ$  relative to the beam direction,  $\sim 1\text{-mg-cm}^{-2}$   $^{208}\text{Pb}$  targets were evaporated onto  $25\text{-mg-cm}^{-2}$  Ni beam stops. To avoid the possible interference from backing-generated projectile x rays, which contribute as a background to the Doppler-shifted projectile x-ray peak, and because the high-energy portion of the detector intrinsic line profile is more easily analyzed, target excitations were studied preferentially when possible. In most cases investigated, x-ray backgrounds from internal conversion, following nuclear excitation, were negligible. The nuclear excitations were monitored by a large-volume Ge(Li) detector. It is important to note also that since the lifetime of the  $K$ -shell vacancies for heavy atoms is much shorter than the slowing-down time in the target (backing), a finite target (backing) thickness does not distort the line shape.

We illustrate the results obtained from two systems studied,  $^{136}\text{Xe} + ^{208}\text{Pb}$  and  $^{238}\text{U} + ^{208}\text{Pb}$  at observation angles of  $0^\circ$  and  $90^\circ$ , in Figs. 1 and 2. For each system, the Pb-target excitation of the  $K\alpha_1$  and  $K\alpha_2$  lines were analyzed. It is clear that the maximum Doppler broadening is an order of magnitude larger than the detector resolution of  $\sim 500$  eV. These specific projectile-target combinations were chosen to isolate approximately both  $1s\sigma$ - and  $2p_{1/2}\sigma$ -related excitations, respectively, by selecting sufficiently asymmetric cases where

vacancy sharing<sup>10</sup> between  $1s\sigma$  and  $2p_{1/2}\sigma$  states is small, as suggested by recent total-cross-section measurements.<sup>11</sup> An untreated spectrum obtained with  $^{136}\text{Xe} + ^{208}\text{Pb}$ , as well as the radiations from collisions with the thick Ni backing normalized to the same integrated beam, are shown in Fig. 1(a) to illustrate the level of the background contribution to the spectra. Also included in Fig. 1(a) is a spectrum of Pb x rays following  $^{208}\text{Bi}$  decay, providing a measure of the line shape for monoenergetic x rays. (At  $90^\circ$ , the shift of  $\sim 300$  eV in centroids between the in-beam and source lines is due to multiple vacancies in the collision.) These source line profiles together with other single line sources were utilized to isolate the photopeak-related fractions of the

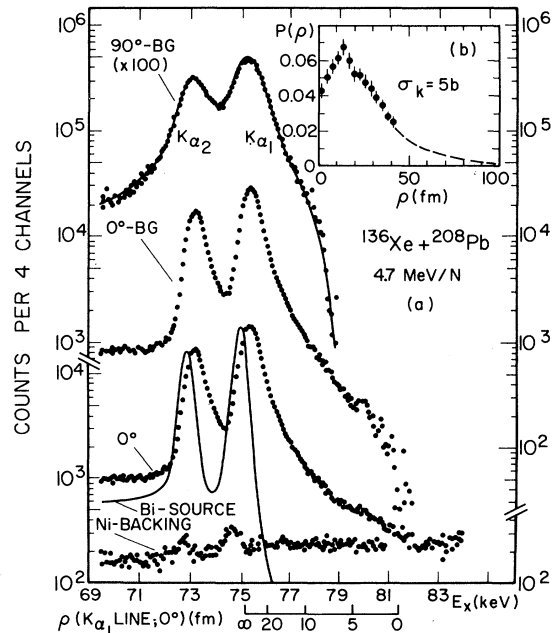


FIG. 1. (a)  $K\alpha_1$ - and  $K\alpha_2$ -line profiles of Pb from  $^{136}\text{Xe} + ^{208}\text{Pb}$  collisions observed at  $0^\circ$  before and after background (BG) subtraction, and at  $90^\circ$  after BG subtraction. Also shown (bottom of figure) is the normalized background from the Ni beam stop, and the  $K\alpha_1$  and  $K\alpha_2$  lines of Pb from  $^{208}\text{Bi}$  decay. The solid line through the  $90^\circ$  spectrum represents the  $90^\circ$  line shape calculated with a  $P(\rho)$  [inset (b)] extracted from the  $0^\circ$  line shape. The dashed line in (b) reflects only mean values of  $P(\rho)$  for the reasons cited in the text.

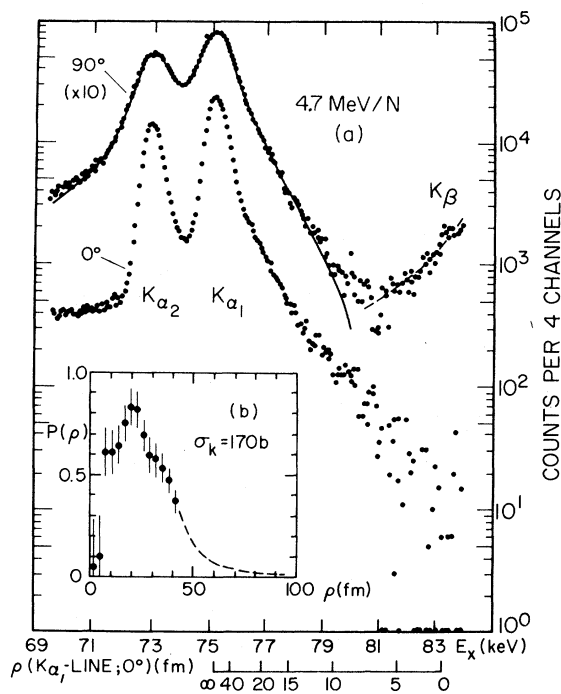


FIG. 2. (a)  $K\alpha_1$ - and  $K\alpha_2$ -line profiles of Pb from  $^{238}\text{U} + ^{208}\text{Pb}$  collisions observed at  $0^\circ$  and  $90^\circ$  after background subtraction. The solid line through the  $90^\circ$  spectrum represents the  $90^\circ$  line shape calculated with a  $P(\rho)$  [inset (b)] extracted from the  $0^\circ$  line shape.

spectra, and in particular, to simulate systematically the low-energy-tail contributions produced by scattering in surrounding material and by incomplete charge collection in the detector. After subtraction of the ambient and beam-induced backgrounds, a progressive unfolding of these tails was carried out for radiations above  $K\alpha_1$  and  $K\alpha_2$  lines to yield the Doppler line profiles and their low-energy tails shown in Figs. 1(a) and 2(a).

The correlation between the photon energy for the  $K\alpha_1$  line and the impact parameter, also included in Figs. 1 and 2, shows that even the qualitative observation of the distinctively broadened line shapes at  $0^\circ$  is an immediate indication of an appreciable contribution to the total cross section from small-impact-parameter collisions. Moreover, an analysis of the symmetry and magnitude of the broadening observed at  $90^\circ$  establishes that these line-broadening effects are Doppler-shift related, and are not produced by continuum emissions or by multiple-charge-state distributions of the decaying atoms.

To obtain a quantitative measure of  $P(\rho)$ , first the  $0^\circ$  photon distributions were deduced by un-

folding the experimental resolution of the detector with an iterative defolding procedure. The location of the unshifted-line centroids were obtained from the  $90^\circ$  data where the Doppler-broadened line shape is symmetric. The resolution function of the detector, modified by a small line broadening due to the satellite structure, was determined by examining the low-energy portion of the  $0^\circ$  line profiles. It is important to point out that the satellite structure produces only small aberrations in determining the average  $P(\rho)$  distributions for  $\rho \lesssim 40$  fm.

$P(\rho)$  was derived from the unfolded  $0^\circ$  photon distribution using Eq. (2) integrated over finite intervals in  $\rho$ . The deduced  $P(\rho)$  are shown in Figs. 1(b) and 2(b). The accuracy of obtaining  $P(\rho)$  for  $\rho \gtrsim 40$  fm diminishes with increasing  $\rho$  because of the uncertainties in determining the centroids and widths of the unshifted line. For  $\rho \gtrsim 100$  fm only the summed cross section is meaningful so that  $P(\rho)$  for these values of  $\rho$  has not been plotted on these graphs. This part of the cross section contributes to the central unshifted part of the line shape. The absolute probability scale is based on measured<sup>11</sup> total cross sections of  $\sigma_K = 5 \pm 3$  b for the Xe + Pb system, and  $170 \pm 60$  for U + Pb. In Figs. 1(a) and 2(a) we also illustrate the simultaneous good fits that are obtained to the  $90^\circ$  data by utilizing  $P(\rho)$  deduced from the  $0^\circ$  distributions. The fact that the reflection of specific impact-parameter scatterings occur in different parts of the line shapes observed at  $0^\circ$  and  $90^\circ$  emphasizes the relevance of the  $90^\circ$  data as a test of the  $P(\rho)$  derived from the  $0^\circ$  line shape.

It is evident from these measurements that the prominent general feature of the impact-parameter dependence for ionization of deeply bound  $1s\sigma$  and  $2p_{1/2}\sigma$  states is a concentration of large excitation probabilities at small impact parameters. Even for the case of  $1s\sigma$  excitation,  $P(\rho)$  near  $\rho = 0$  is as large as a few percent. Moreover,  $(43 \pm 5)\%$  of this total cross is contributed by collisions with  $\rho \lesssim 40$  fm. In general agreement with the predictions by Betz *et al.*,<sup>3</sup> both these observations indicate that  $1s\sigma$  vacancy formation is considerably more favorable for observing the spontaneous and induced emission of positrons<sup>2</sup> than suggested by the earlier pessimistic estimates for  $P(\rho = 0)$  of  $(10^{-3} - 10^{-2})\%$ .<sup>4,5</sup>

In addition to these main conclusions, an examination of the detailed features of  $P(\rho)$  also provides interesting information on aspects of the excitation process. In particular, the posi-

tive slopes observed for  $P(\rho)$  near  $\rho=0$  in Figs. 1(b) and 2(b) imply that the radial coupling assumed by Betz *et al.*<sup>3</sup> cannot be the only source of excitation, since for this mechanism the slope of  $P(\rho)$  is expected to be zero for  $\rho=0$ .<sup>3</sup> In fact, these  $P(\rho)$  distributions suggest that a rotational-coupling mechanism may be involved also. It is of considerable interest to explore these questions in detail. We have demonstrated that the Doppler-shift technique introduced in these experiments provides such an opportunity.

We thank Professor W. Greiner, Professor B. Müller, and Dr. G. Soff for many valuable discussions, and Dr. R. Simon and Dr. H. T. Wollersheim for their assistance. One of the authors (J.S.G.), wants to express his gratitude to the GSI laboratory for the hospitality extended to him, and to the Alexander von Humboldt-Stiftung for support under a Senior U. S. Scientist Award.

<sup>1</sup>H. Backe, E. Berdermann, H. Bokemeyer, J. S. Greenberg, E. Kankeleit, P. Kienle, Ch. Kozhuharov, L. Handschug, Y. Nakayama, L. Richter, H. Stettmier, F. Weik, and R. Willwater, in *Proceedings of the Tenth International Conference on the Physics of Electronic*

*and Atomic Collisions, Paris, 1977* (Commissariat à l'Énergie Atomique, Paris), p. 162.

<sup>2</sup>K. Smith, H. Peitz, B. Müller, and W. Greiner, *Phys. Rev. Lett.* **32**, 554 (1974).

<sup>3</sup>W. Betz, G. Soff, B. Müller, and W. Greiner, *Phys. Rev. Lett.* **37**, 1046 (1976).

<sup>4</sup>C. Foster, T. R. Hoogkammer, P. Woerlee, and F. W. Saris, *J. Phys. B* **9**, 1943 (1976).

<sup>5</sup>W. E. Meyerhof, *Phys. Rev. A* **10**, 1005 (1974).

<sup>6</sup>D. Schwalm, A. Bamberger, P. G. Bizzeti, B. Povh, G. A. P. Engelbertnik, J. W. Olness, and E. K. Warburton, *Nucl. Phys. A* **192**, 449 (1972).

<sup>7</sup>J. S. Greenberg, H. Bokemeyer, H. Emling, E. Grosse, D. Schwalm, and H. J. Wollersheim, in *Proceedings of the Tenth International Conference on the Physics of Electronic and Atomic Collisions, Paris, 1977* (Commissariat à l'Énergie Atomique, Paris), p. 160.

<sup>8</sup>R. Anholt, to be published.

<sup>9</sup>H. H. Behncke, P. Armbruster, F. Folkmann, S. Hagmann, and P. H. Mokler, in *Proceedings of the Tenth International Conference on the Physics of Electronic and Atomic Collisions, Paris, 1977* (Commissariat à l'Énergie Atomique, Paris), p. 158.

<sup>10</sup>W. E. Meyerhof, *Phys. Rev. Lett.* **31**, 1341 (1973).

<sup>11</sup>H. H. Behncke, P. Armbruster, F. Folkmann, S. Hagmann, and P. H. Mokler, in *Proceedings of the Tenth International Conference on the Physics of Electronic and Atomic Collisions, Paris, 1977* (Commissariat à l'Énergie Atomique, Paris), p. 156.

## Particle-Caviton Interactions

A. Y. Wong, P. Leung, and D. Eggleston

*Department of Physics, University of California, Los Angeles, California 90024*

(Received 10 August 1977)

Experiments using a controlled electron beam interacting with a caviton containing coherent rf fields demonstrate the importance of transit-time damping of localized high-frequency fields. A small transverse magnetic field ( $B \leq 10$  G,  $\omega_c/\omega_p \leq 0.1$ ) was sufficient to eliminate such transit-time damping. A modulated electron beam is used to demonstrate that the interaction between the beam and the caviton field is phase sensitive. Regeneration of cavitons by streaming particles is discussed.

We wish to report experiments which demonstrate that localized oscillating fields together with their density perturbations (hereafter referred to as cavitons<sup>1</sup>) are sensitively dependent on the ambient background electron distribution function. Our experiments consist of monitoring the amplitude of the localized electric field of the caviton in the presence of an electron distribution whose fast-electron population can be controlled. Our results agree with recent theoretical studies<sup>2-4</sup> on the effective energy exchange between cavitons and particles and the role of

this interaction in determining the saturation value of localized fields.

Our first experiment is performed in a modified double-plasma device.<sup>1,5</sup> A density gradient is formed in the target side by arranging the filaments preferentially. Our operation conditions are  $kT_e \approx 2$  eV,  $T_e/T_i \approx 10$ ,  $n \approx 10^9$  cm<sup>-3</sup>,  $n_0/\nabla n_0 \approx 25$  cm, and  $\gamma_{en}/\omega_p \approx 10^{-3}$ . A quasistatic external rf field ( $\omega_0/2\pi \approx 300$  MHz) is imposed on the plasma by applying a signal to an antenna located at the low-density side of the chamber ( $\xi_0 \approx 3$  V/cm). At the resonance region an intense local-